Adiabatic calorimetry data from ARSST scan

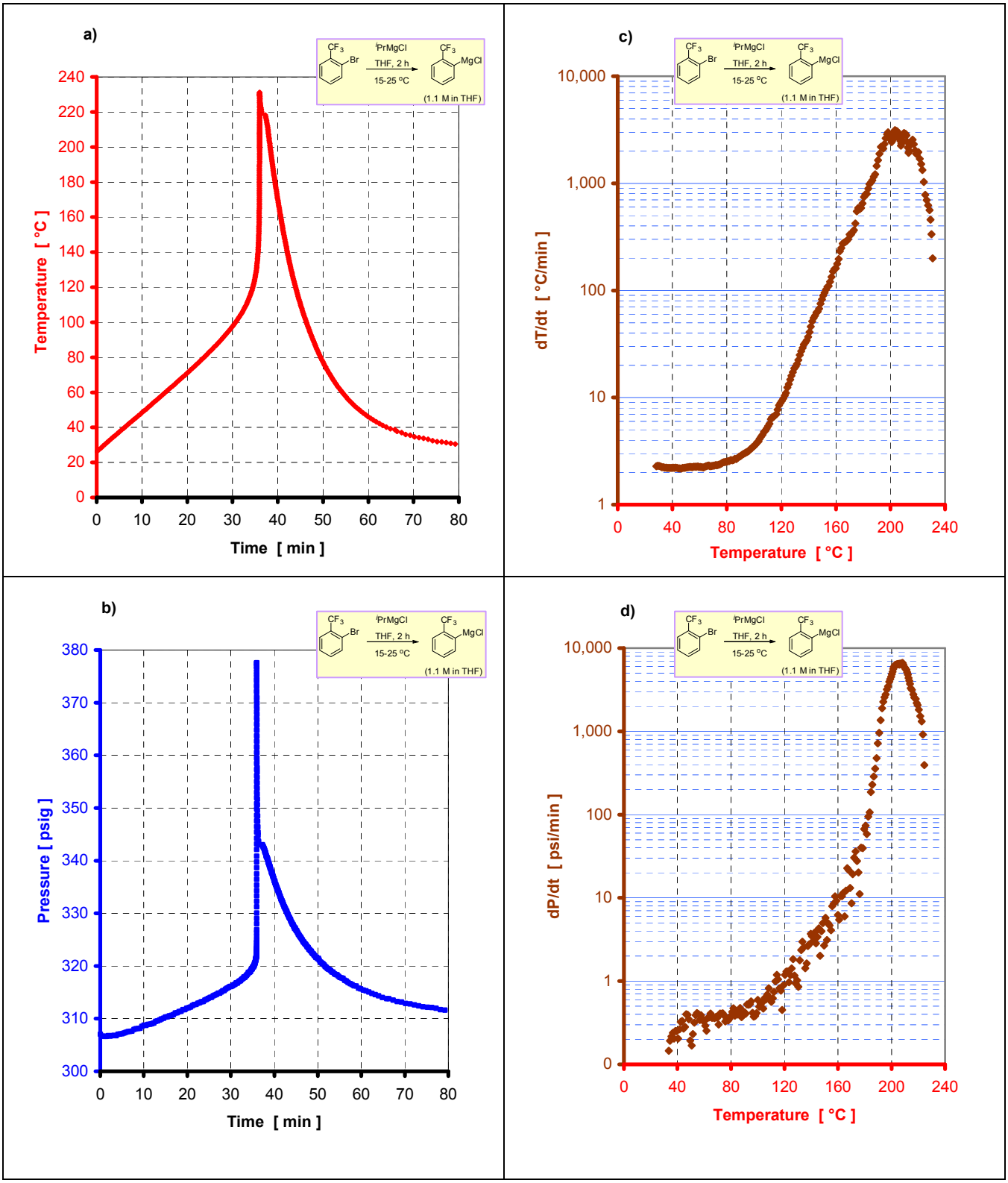

Figure 1. Formation of 2-trifluoromethylphenyl magnesium chloride (1.1 M). Data from ARSST quasi adiabatic calorimetry: a) Temperature vs Time plot; b) Pressure vs Time plot; c) Time derivative of Temperature (temperature rise rate) vs Temperature plot (log. scale); d) Time derivative of Pressure (pressure rise rate) vs Temperature plot (log. scale). Both the heat-up and cool down portions are shown in a) and b). Only the heat-up portion is shown in c) and d).

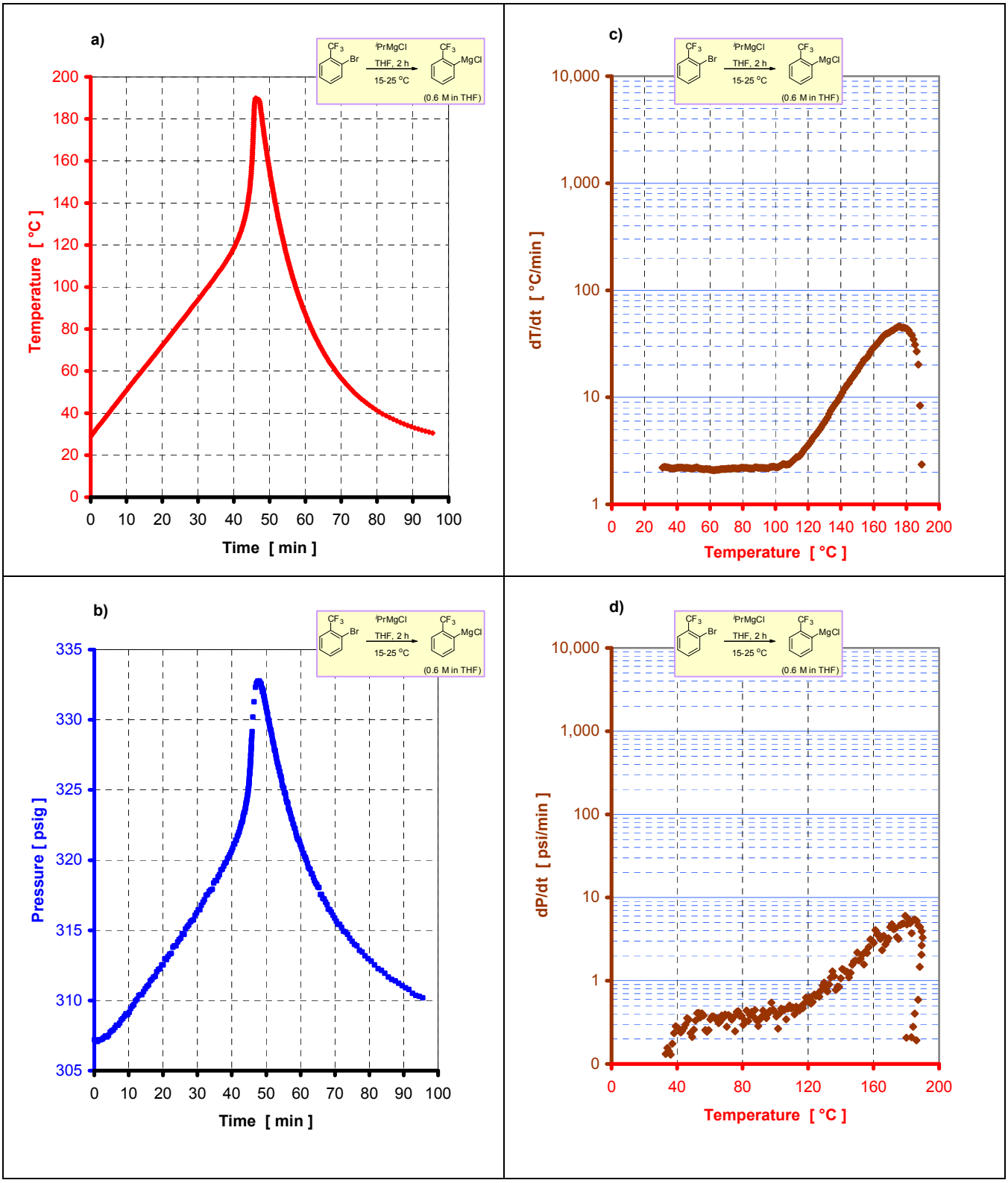

Figure 2. Formation of 2-trifluoromethylphenyl magnesium chloride (0.6 M). Data from ARSST quasi adiabatic calorimetry: a) Temperature vs Time plot; b) Pressure vs Time plot; c) Time derivative of Temperature (temperature rise rate) vs Temperature plot (log. scale); d) Time derivative of Pressure (pressure rise rate) vs Temperature plot (log. scale). Both the heat-up and cool down portions are shown in a) and b). Only the heat-up portion is shown in c) and d).

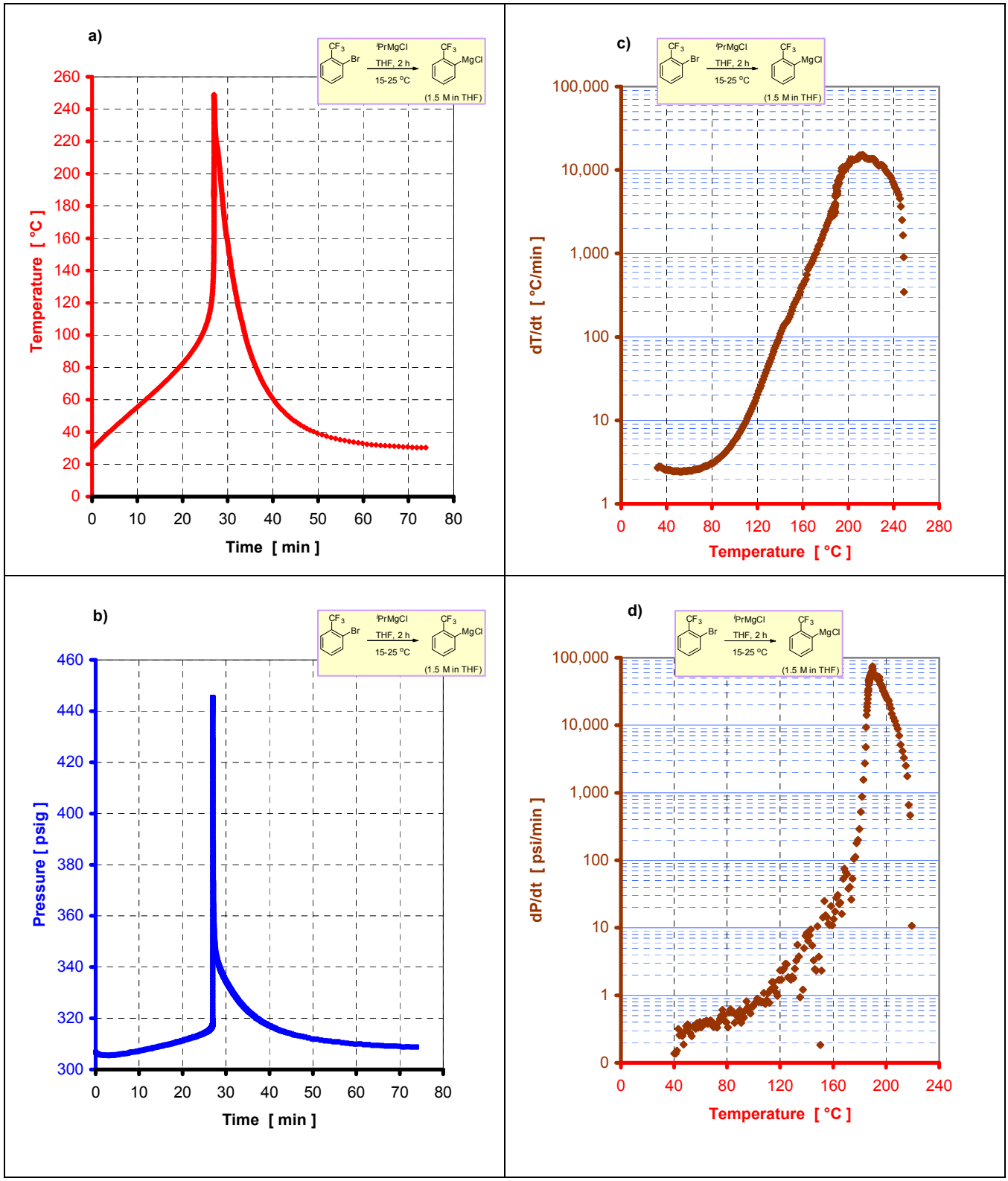

Figure 3. Formation of 2-trifluoromethylphenyl magnesium chloride (1.5 M). Data from ARSST quasi adiabatic calorimetry: a) Temperature vs Time plot; b) Pressure vs Time plot; c) Time derivative of Temperature (temperature rise rate) vs Temperature plot (log. scale); d) Time derivative of Pressure (pressure rise rate) vs Temperature plot (log. scale). Both the heat-up and cool down portions are shown in a) and b). Only the heat-up portion is shown in c) and d).

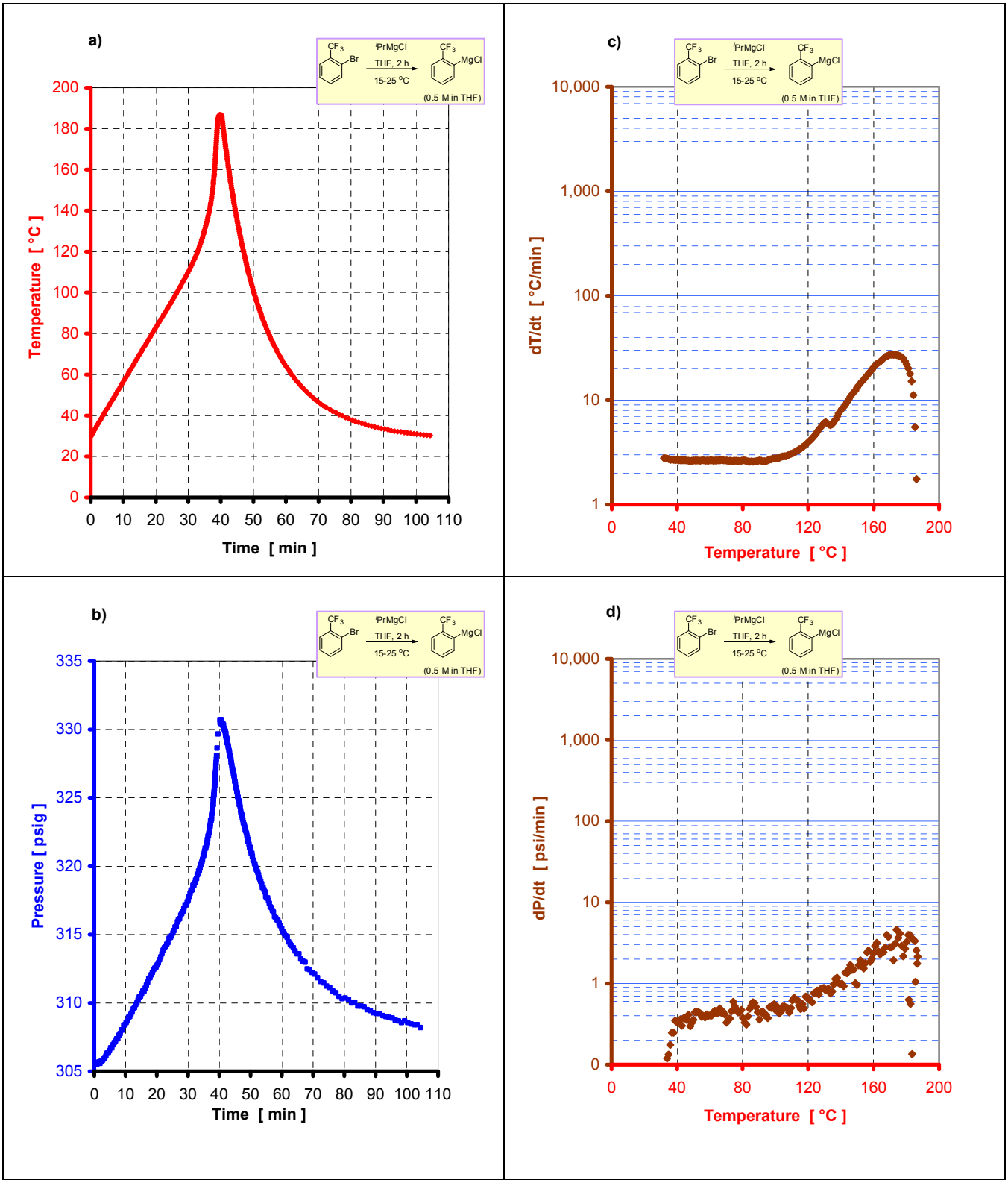

Figure 4. Formation of 2-trifluoromethylphenyl magnesium chloride (0.5 M). Data from ARSST quasi adiabatic calorimetry: a) Temperature vs Time plot; b) Pressure vs Time plot; c) Time derivative of Temperature (temperature rise rate) vs Temperature plot (log. scale); d) Time derivative of Pressure (pressure rise rate) vs Temperature plot (log. scale). Both the heat-up and cool down portions are shown in a) and b). Only the heat-up portion is shown in c) and d).

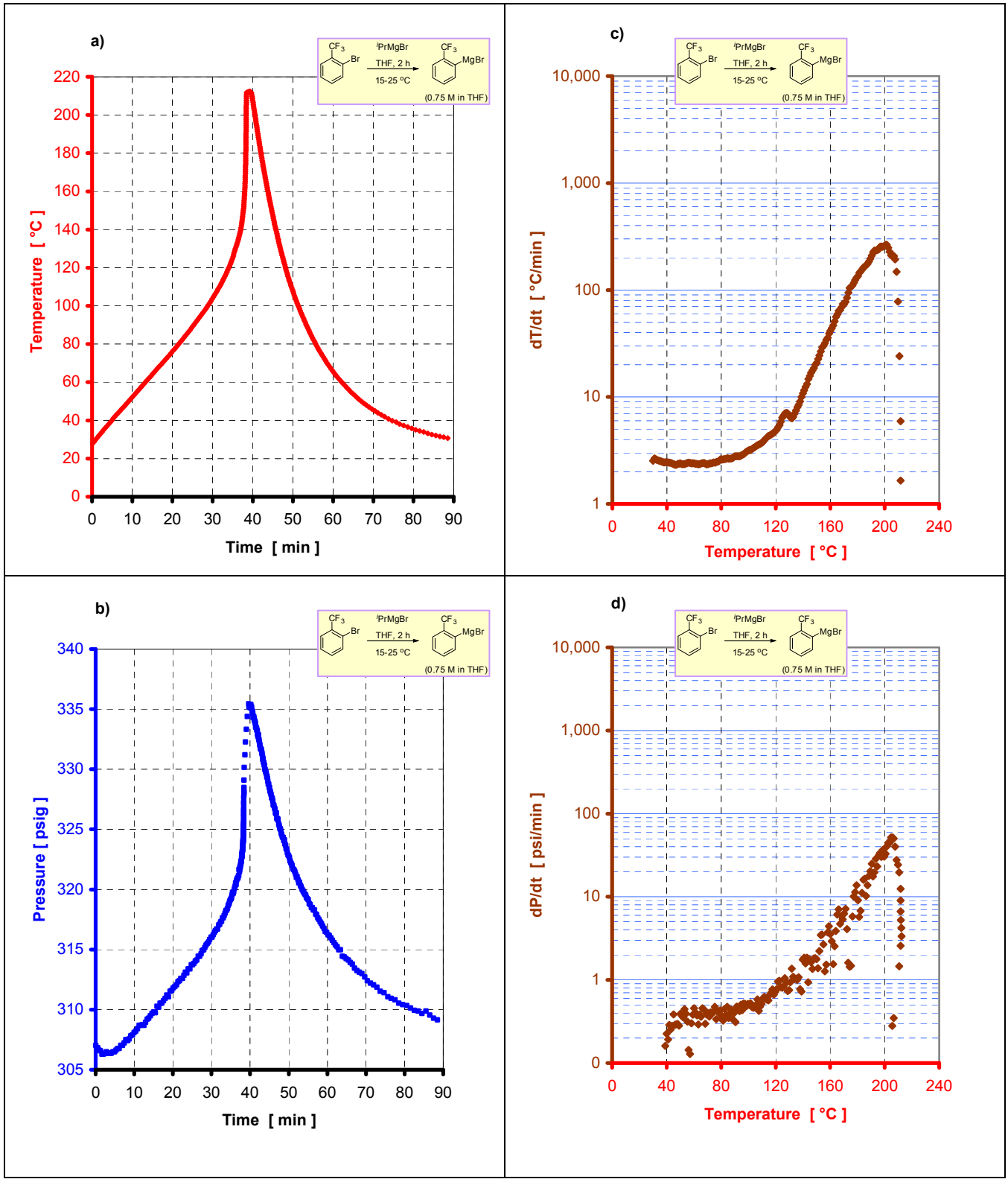

Figure 5. Formation of 2-trifluoromethylphenyl magnesium bromide (0.75 M). Data from ARSST quasi adiabatic calorimetry: a) Temperature vs Time plot; b) Pressure vs Time plot; c) Time derivative of Temperature (temperature rise rate) vs Temperature plot (log. scale); d) Time derivative of Pressure (pressure rise rate) vs Temperature plot (log. scale). Both the heat-up and cool down portions are shown in a) and b). Only the heat-up portion is shown in c) and d).

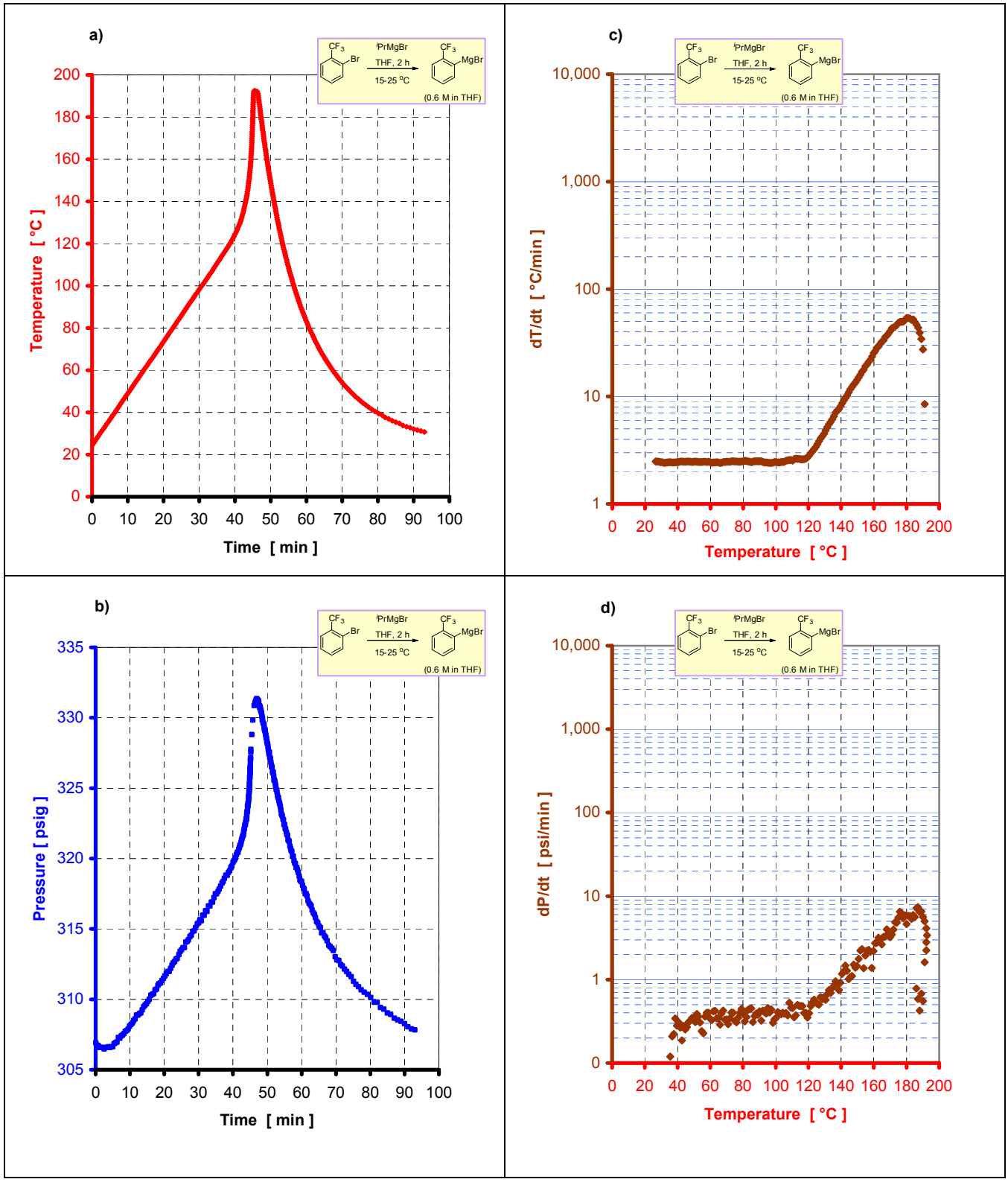

Figure 6. Formation of 2-trifluoromethylphenyl magnesium bromide (0.6 M). Data from ARSST quasi adiabatic calorimetry: a) Temperature vs Time plot; b) Pressure vs Time plot; c) Time derivative of Temperature (temperature rise rate) vs Temperature plot (log. scale); d) Time derivative of Pressure (pressure rise rate) vs Temperature plot (log. scale). Both the heat-up and cool down portions are shown in a) and b). Only the heat-up portion is shown in c) and d).

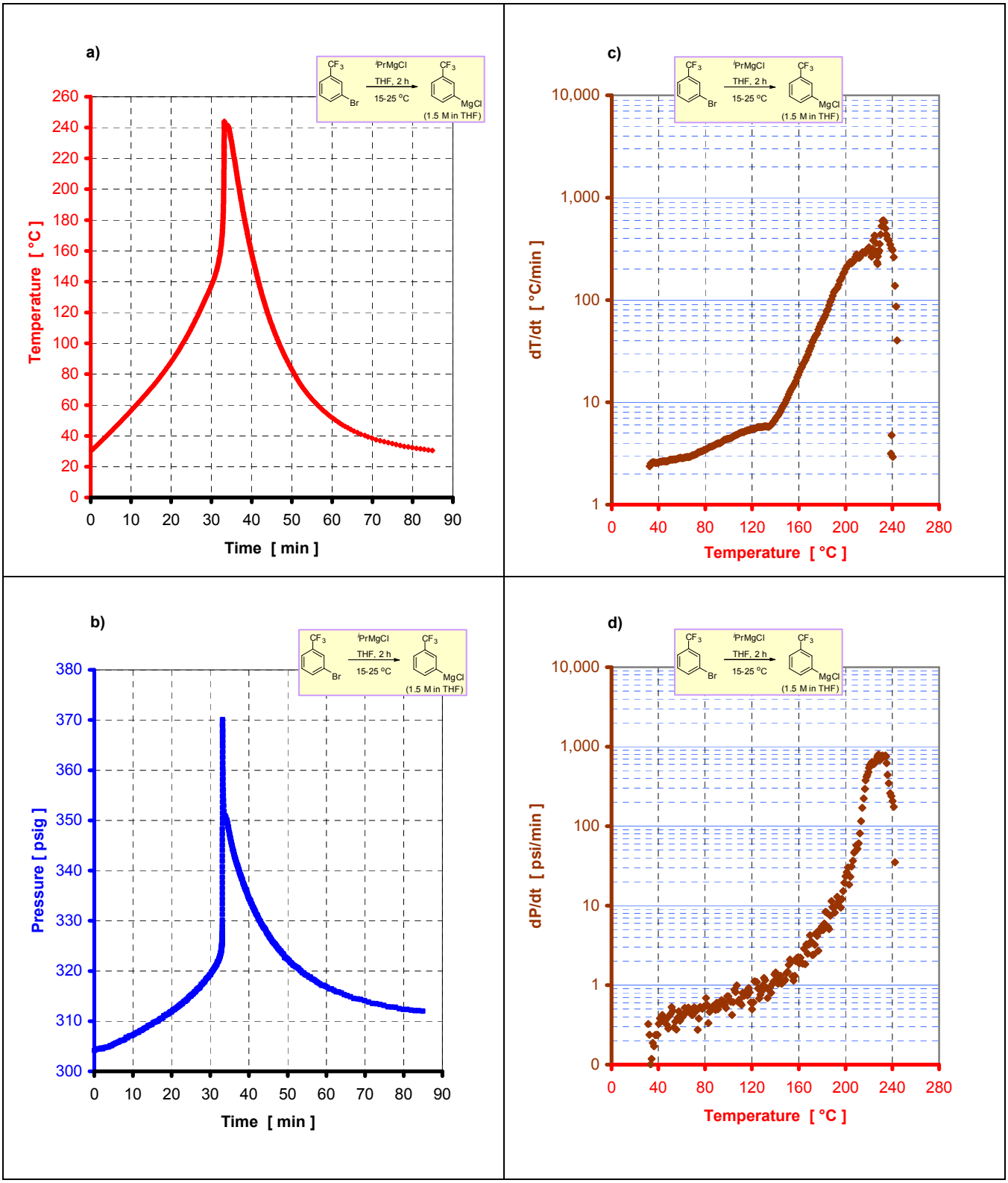

Figure 7. Formation of 3-trifluoromethylphenyl magnesium chloride (1.5 M). Data from ARSST quasi adiabatic calorimetry: a) Temperature vs Time plot; b) Pressure vs Time plot; c) Time derivative of Temperature (temperature rise rate) vs Temperature plot (log. scale); d) Time derivative of Pressure (pressure rise rate) vs Temperature plot (log. scale). Both the heat-up and cool down portions are shown in a) and b). Only the heat-up portion is shown in c) and d).

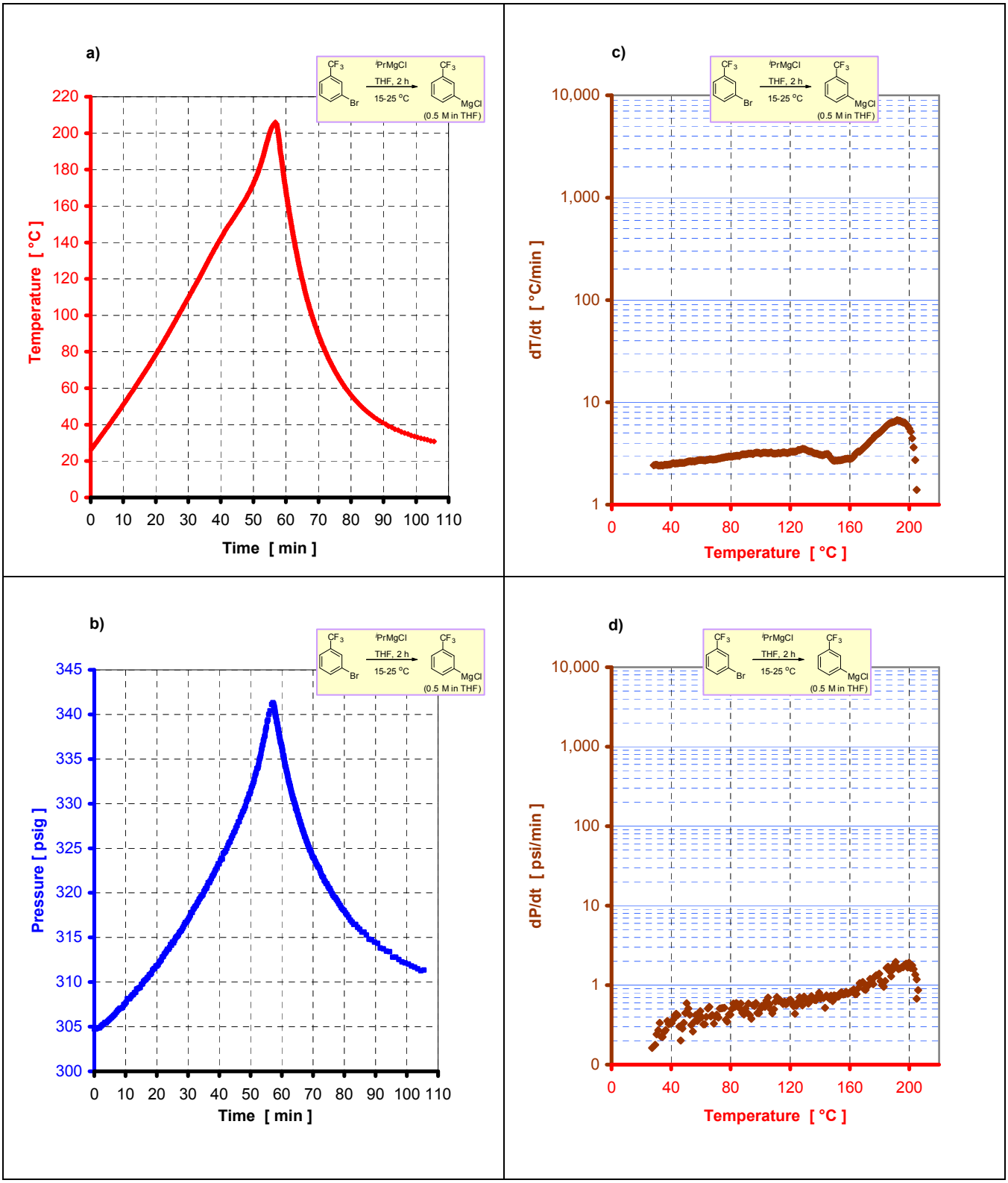

Figure 8. Formation of 3-trifluoromethylphenyl magnesium chloride (0.5 M). Data from ARSST quasi adiabatic calorimetry: a) Temperature vs Time plot; b) Pressure vs Time plot; c) Time derivative of Temperature (temperature rise rate) vs Temperature plot (log. scale); d) Time derivative of Pressure (pressure rise rate) vs Temperature plot (log. scale). Both the heat-up and cool down portions are shown in a) and b). Only the heat-up portion is shown in c) and d).

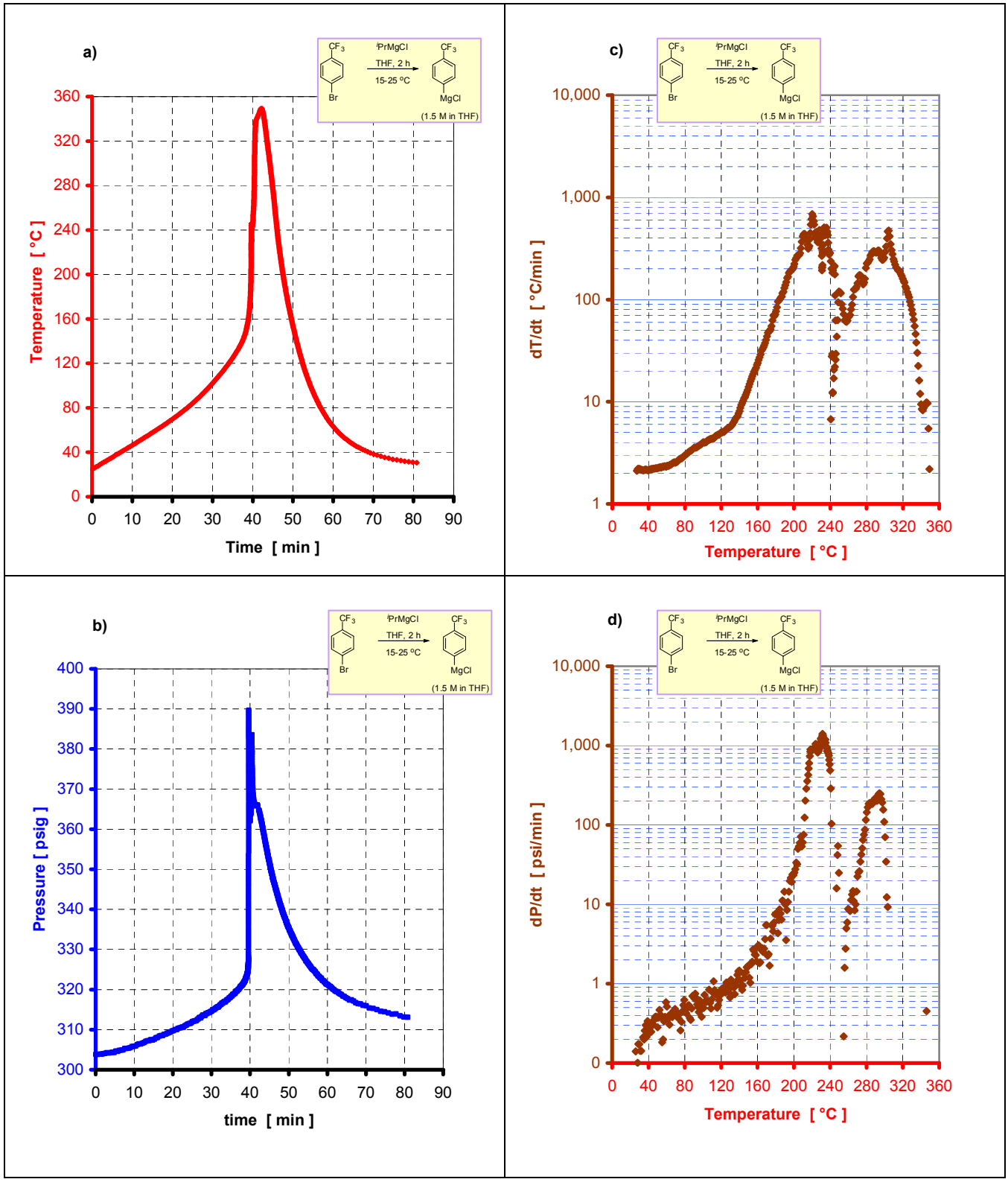

Figure 9. Formation of 4-trifluoromethylphenyl magnesium chloride (1.5 M). Data from ARSST quasi adiabatic calorimetry: a) Temperature vs Time plot; b) Pressure vs Time plot; c) Time derivative of Temperature (temperature rise rate) vs Temperature plot (log. scale); d) Time derivative of Pressure (pressure rise rate) vs Temperature plot (log. scale). Both the heat-up and cool down portions are shown in a) and b). Only the heat-up portion is shown in c) and d).

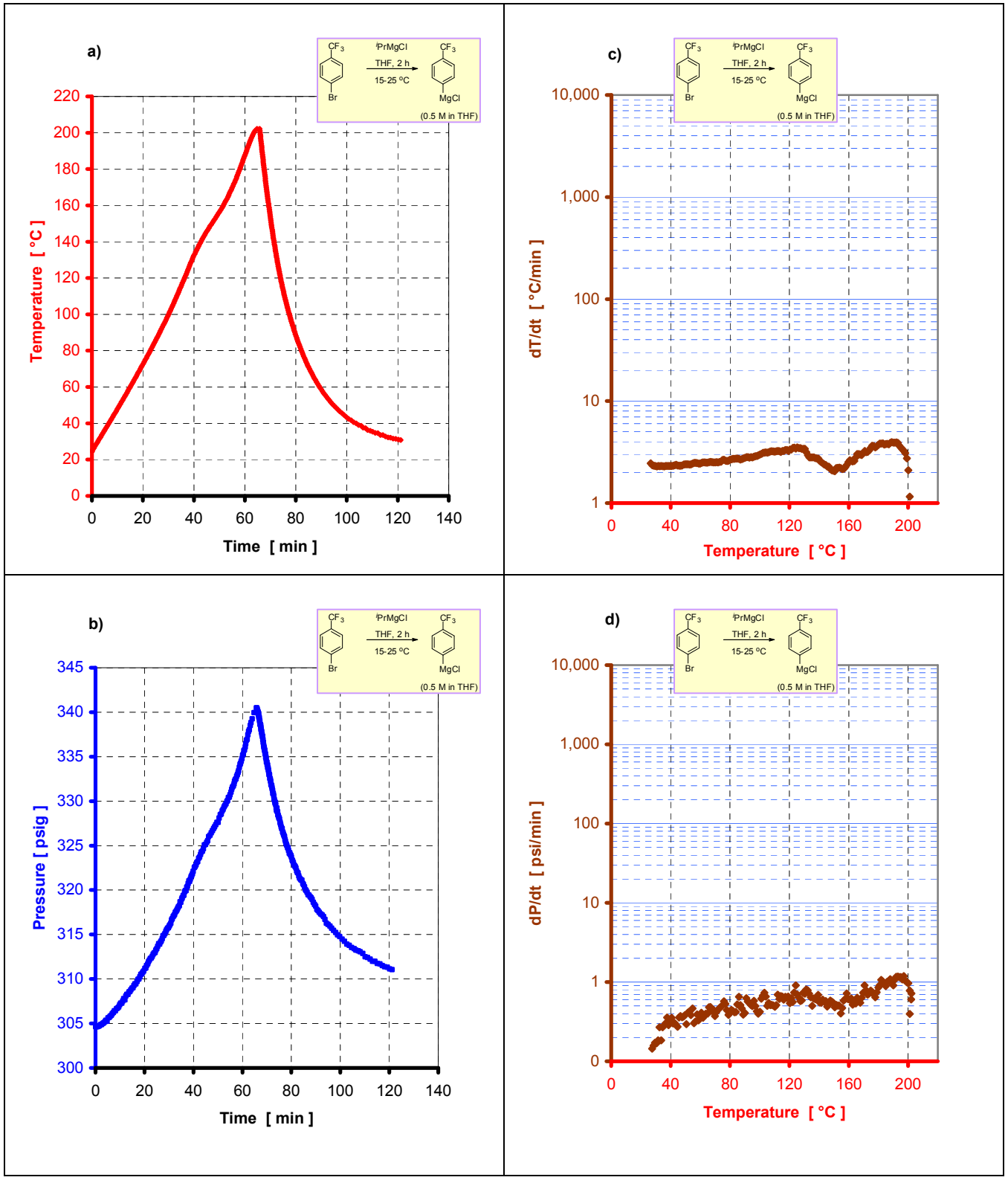

Figure 10. Formation of 4-trifluoromethylphenyl magnesium chloride (0.5 M). Data from ARSST quasi adiabatic calorimetry: a) Temperature vs Time plot; b) Pressure vs Time plot; c) Time derivative of Temperature (temperature rise rate) vs Temperature plot (log. scale); d) Time derivative of Pressure (pressure rise rate) vs Temperature plot (log. scale). Both the heat-up and cool down portions are shown in a) and b). Only the heat-up portion is shown in c) and d).

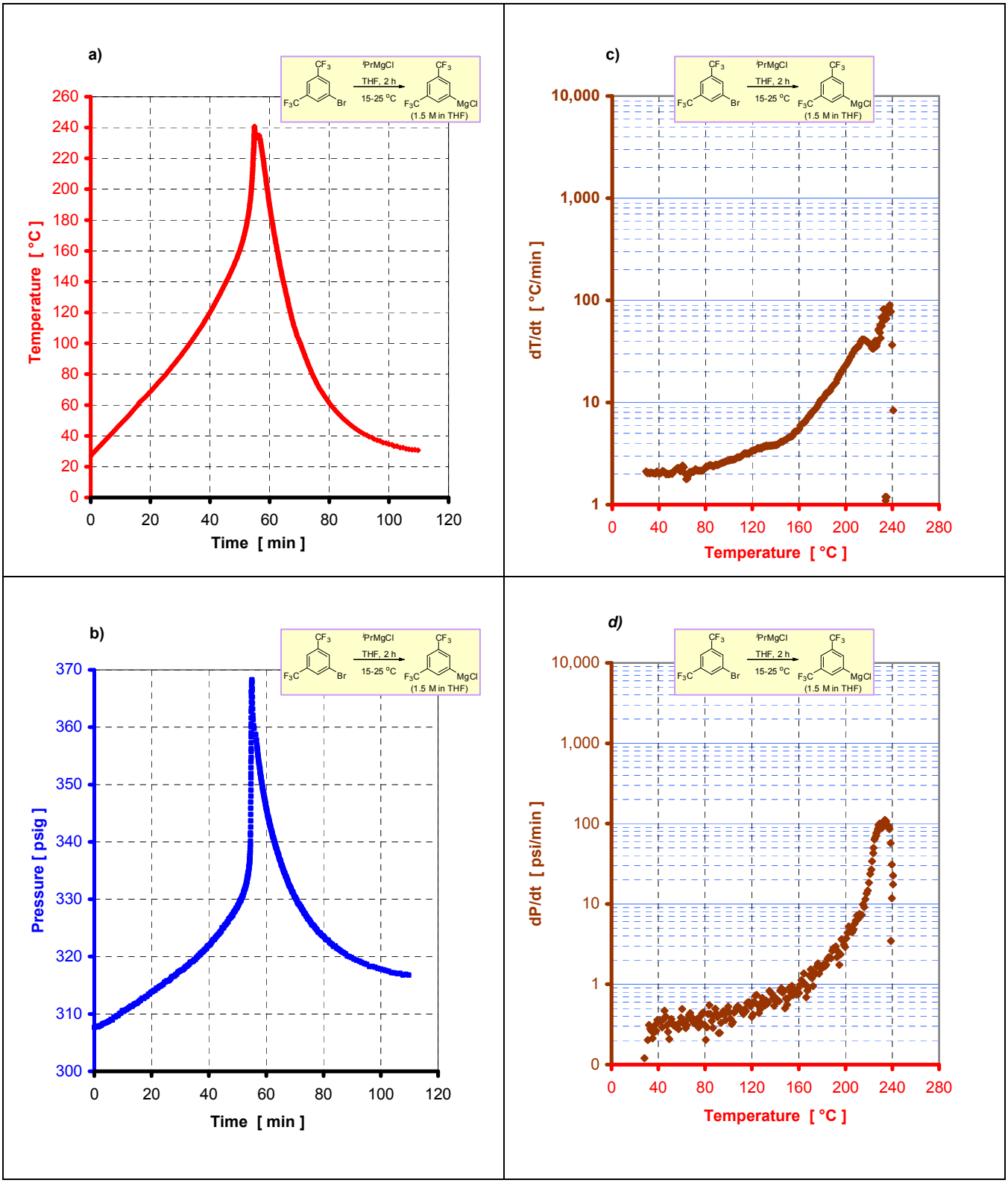

Figure 11. Formation of 3,5-di-trifluoromethylphenyl magnesium chloride (1.5 M). Data from ARSST quasi adiabatic calorimetry: a) Temperature vs Time plot; b) Pressure vs Time plot; c) Time derivative of Temperature (temperature rise rate) vs Temperature plot (log. scale); d) Time derivative of Pressure (pressure rise rate) vs Temperature plot (log. scale). Both the heat-up and cool down portions are shown in a) and b). Only the heat-up portion is shown in c) and d).

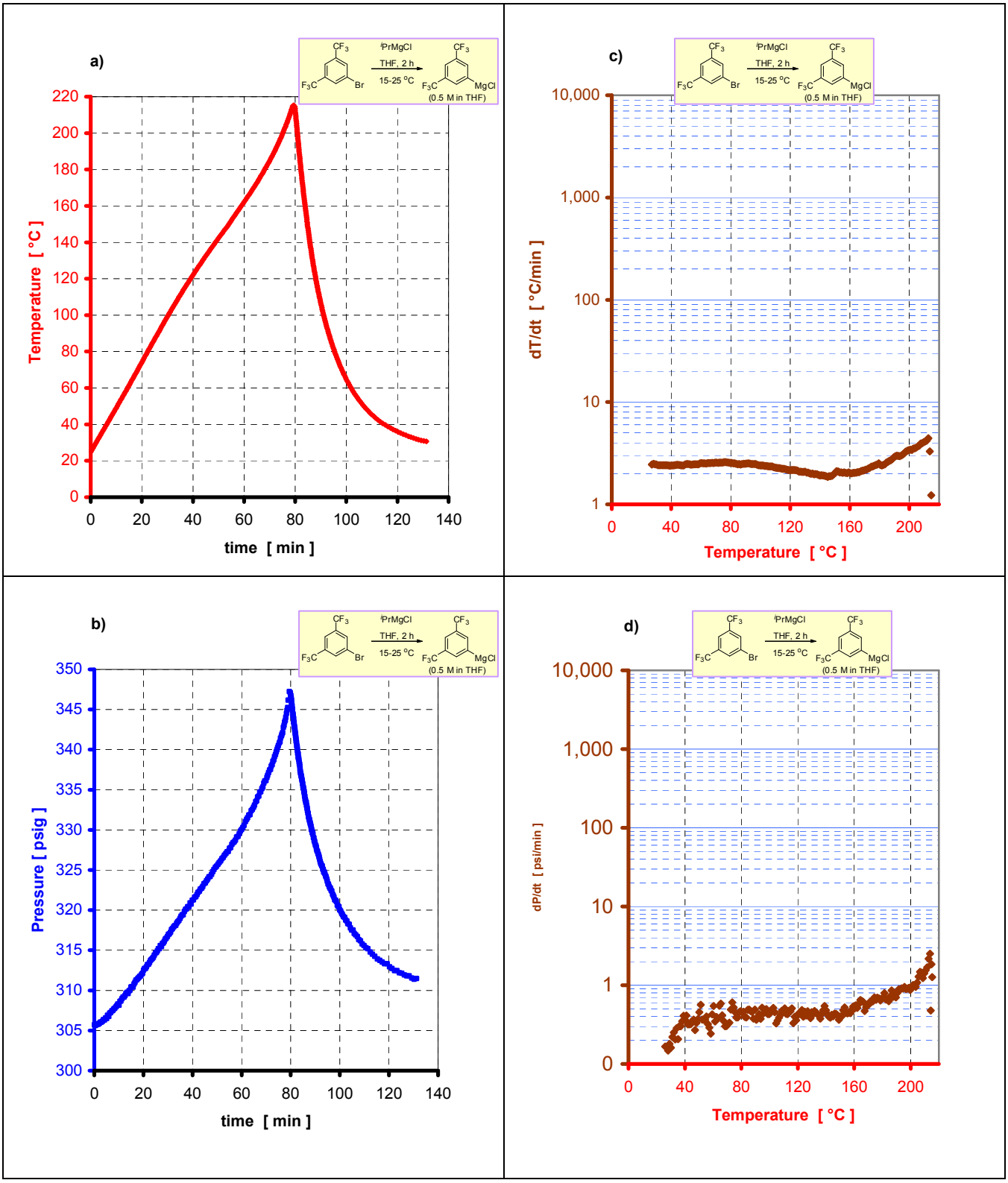

Figure 12. Formation of 3,5-di-trifluoromethylphenyl magnesium chloride (0.5 M). Data from ARSST quasi adiabatic calorimetry: a) Temperature vs Time plot; b) Pressure vs Time plot; c) Time derivative of Temperature (temperature rise rate) vs Temperature plot (log. scale); d) Time derivative of Pressure (pressure rise rate) vs Temperature plot (log. scale). Both the heat-up and cool down portions are shown in a) and b). Only the heat-up portion is shown in c) and d).

Determination of the total fluorine content: The total fluorine content of the decomposition products is measured by ISE elemental analysis. The sample is accurately weighed and transferred to a bed of mannitol wrapped in an ashless filter paper. The sample is combusted in an oxygen combustion flask containing 100 ml of TISAB II where the covalently bound fluorine is converted to fluoride. The sample is set aside for 20 minutes. Fluorine in organic materials is determined by transferring the quench solution to a sample beaker which is then analyzed potentiometrically by an ion specific electrode using a single known addition technique. The system is checked with an NIST traceable organic standard, which contains fluorine, prior to sample analysis. The standard is checked to within +0.3% absolute. %F is calculated based on the sample weight, solution volume and fluoride concentration.

Determination of the fluoride ion content: The fluoride ion content of the decomposition products is measured by ion chromatography. The sample is weighed accurately into an aluminum sample boat and transferred into an appropriate size volumetric flask. The sample is dissolved to volume using the mobile phase as the diluent. If necessary, a small amount of methanol is added to aid dissolution. Additionally, cloudy sample solutions are filtered through a nylon syringe filter prior to analysis. The sample solutions are analyzed by ion chromatography using a polymeric anion exchange resin and a sodium carbonate/sodium hydrogen carbonate mobile phase. The sample solution is injected into the ion exchange column using a liquid pump and liquid autosampler. In the column, the ions are separated as they exchange between the mobile phase and stationary phase. Ions are detected as they elute from the end of the column by a conductivity detector. This detector measures the electrical conductivity of the solution eluting from the column and generates a response proportional to the concentration of ions in the solution. To increase the sensitivity of the detector, the background conductivity due to the mobile phase is suppressed by neutralization with counter ions. Anions in the sample are identified and quantified by comparison to known standard solutions. The system is calibrated using diluted standard solutions prepared from NIST traceable standard solutions. System suitability and standard confirmation are demonstrated from replicate injections of a working standard solution and a check standard solution prior to injections of the sample solutions. The working standard solution is also injected and evaluated periodically throughout the sequence and at the end of the sequence to ensure that the system suitability is maintained.

Both the fluoride content and the total fluorine content of the decomposition products of 2-trifluoromethylphenyl magnesium chloride in THF at various concentrations were analyzed by using the above methods and the results are shown in Table 1.

Table 1. Fluorine analysis of the decomposition products of 2-trifluoromethylphenyl magnesium chloride in THF

	Decomposition products of 2-trifluoromethylphenyl magnesium chloride in THF at various concentration			
	1.5 M	1.1 M	0.6 M	0.5 M
Total fluorine content (F% w/w)	9.74	7.80	4.68	3.90
Fluoride content (F-% w/w)	2.45	2.12	1.73	1.42
F-%/F%	0.25	0.27	0.36	0.36